J Biomol NMR (2009) 43:51–61
DOI 10.1007/s10858-008-9292-9

ARTICLE

Design of high-power, broadband 180° pulses and mixing sequences for fast MAS solid state chemical shift correlation NMR spectroscopy

Christian Herbst · Jirada Herbst · Anika Kirschstein · Jörg Leppert · Oliver Ohlenschläger · Matthias Görlach · Ramadurai Ramachandran

Received: 16 July 2008 / Accepted: 28 October 2008 / Published online: 19 November 2008
© Springer Science+Business Media B.V. 2008

Abstract An approach for the design of high-power, broadband 180° pulses and mixing sequences for generating dipolar and scalar coupling mediated ^{13}C–^{13}C chemical shift correlation spectra of isotopically labelled biological systems at fast magic-angle spinning frequencies without ^{1}H decoupling during mixing is presented. Considering RF field strengths in the range of 100–120 kHz, as typically available in MAS probes employed at high spinning speeds, and limited B_1 field inhomogeneities, the Fourier coefficients defining the phase modulation profile of the RF pulses were optimised numerically to obtain broadband inversion and refocussing pulses and mixing sequences. Experimental measurements were carried out to assess the performance characteristics of the mixing sequences reported here.

Introduction

Magic angle spinning solid state NMR is becoming a powerful tool for biomolecular structural investigations in general and in particular for systems that are difficult to study by conventional solution state NMR or by X-ray crystallography (Castellani et al. 2002; Jaroniec et al. 2002; Rienstra et al. 2002; Luca et al. 2003; Tycko 2003; Krabben et al. 2004; Leppert et al. 2004; Zech et al. 2005; Riedel et al. 2005, 2006; Goldbourt et al. 2007; Zhou et al. 2007). The pre-requisite for any NMR based structural investigation is the sequence specific assignment of resonances and the extraction of distance and torsion angle constraints. The characteristic connectivity patterns seen in a ^{13}C–^{13}C chemical shift correlation spectrum is commonly exploited to assign the carbon resonances belonging to a specific class of residue, e.g. to a particular type of amino acid in a peptide/protein or to a sugar residue in nucleic acids. Although weak dipolar couplings between low γ nuclei are normally lost under fast magic angle spinning, efficient dipolar recoupling schemes have been developed for inhibiting the spatial averaging of dipolar couplings in rotating solids (Levitt 2002). This has made possible the generation of broadband ^{13}C–^{13}C chemical shift correlation spectra and the assignment of ^{13}C resonances in isotopically labelled biological systems. Mixing schemes based on homonuclear scalar couplings, in contrast to dipolar couplings, can lead to a complete transfer of magnetisation from one spin to another in a two spin system and, hence, to improved crosspeak intensities (Baldus and Meier 1996; Heindrichs et al. 2001; Hardy et al. 2003). The performance of scalar coupling based sequences is also not affected by molecular mobility. Not surprisingly, through-bond scalar-coupling mediated ^{13}C–^{13}C MAS chemical shift correlation spectroscopy (TOBSY), in addition to through-space dipolar-driven correlation experiments, has been found to be an useful complementary tool for unambiguous resonance assignments (Detken et al. 2001; Ernst et al. 2003).

Many of the dipolar and scalar coupling based mixing schemes reported in the literature make extensive use of

C. Herbst · A. Kirschstein · J. Leppert · O. Ohlenschläger · M. Görlach · R. Ramachandran (✉)
Research group Biomolecular NMR spectroscopy, Leibniz Institute for Age Research, Fritz Lipmann Institute, 07745 Jena, Germany
e-mail: raman@fli-leibniz.de

J. Herbst
Department of Mathematics, Statistics and Computer, Faculty of Science, Ubon Ratchathani University, 34190 Ubon Ratchathani, Thailand

180° pulses. For example, Levitt and co-workers have developed an elegant symmetry-based approach for the design of MAS solid state NMR RF pulse schemes for effecting the evolution of the spins under the desired average Hamiltonian of interest (Levitt 2002). Two classes of symmetry-based sequences, denoted as CN_n^v and RN_n^v, have found extensive applications till date. The CN_n^v class of RF pulse schemes involves the application of a basic element "*C*" corresponding to an RF cycle with unity propagator $U_{RF}(\tau_c) = \pm 1$. *N* such cycles are applied over *n* rotor periods τ_r with successive *C* elements incremented in phase by $v2\pi/N$. Basic *C* elements are commonly constructed by suitable concatenation of 180° pulses, e.g. $\{x\bar{x}\}$ and $\{xx\bar{x}\bar{x}\}$. In the RN_n^v scheme, the basic component is a 180° pulse "*R*". A pair of appropriately phase-shifted pulses are derived from this basic element to form a RF pulse sandwich "**R**" and this pulse sandwich is repeated *N*/2 times over *n* rotor periods so as to form an RF cycle with unity propagator $U_{RF}(\tau_c) = \pm 1$. *N, n* and *v* are all integers and appropriate values for these are chosen, via the selection rule for CN_n^v and RN_n^v symmetry, to generate the desired average Hamiltonian. At a given spinning speed, for generating the desired mixing Hamiltonian, it is possible, *in principle*, to employ a variety of symmetry-based sequences together with basic "*C*" or "*R*" elements of different durations. For example, at a spinning speed of 33.333 kHz and with basic *C* elements of the type $\{x\bar{x}\}$ and $\{xx\bar{x}\bar{x}\}$, CN_n^v sequences for achieving magnetisation transfer through homonuclear *J*-couplings can be realised employing 180° pulses with durations in the range of 10–25 μs: $C9_{15}^1$ (25.0 μs, $x\bar{x}$); $C9_{12}^1$ (20.0 μs, $x\bar{x}$) and $C9_{15}^1$ (12.50 μs, $xx\bar{x}\bar{x}$) (Levitt 2002; Hardy et al. 2003). The performance of the sequences, in general, critically depends on the choice of the basic element. Typically, homonuclear chemical shift correlation experiments are carried out with the application of high-power ^{1}H decoupling during mixing. However, recent studies have shown that it is possible to completely eliminate the interference between the decoupling and recoupling RF fields by carrying out these experiments more elegantly in the absence of ^{1}H decoupling with sequences designed to not only recouple the ^{13}Cs, but also simultaneously decouple the ^{1}H spins (Hughes et al. 2004; Marin-Montesinos et al. 2005; De Paepe et al. 2005; Mou et al. 2006; Riedel et al. 2007; Herbst et al. 2007; Bayro et al. 2008). Such sequences, which are of interest in this study, can be implemented using simple rectangular 180° pulses (Bayro et al. 2008), composite pulses (Hughes et al. 2004; Mou et al. 2006) and adiabatic inversion pulses (Riedel et al. 2007; Herbst et al. 2007). For example, the possibility to generate scalar coupling mediated ^{13}C–^{13}C chemical shift correlation spectra without ^{1}H decoupling during mixing has been demonstrated (Mou et al. 2006) employing the $R30_6^{14}$ symmetry-based RF pulse scheme with the basic *R* element $(90)_x(270)_{-x}$, using an RF field strength that is 5 times the spinning speed employed. Such dependences of the required RF field strength on the spinning speed can limit the applicability of these sequences at very fast MAS frequencies. One of the advantages in employing adiabatic inversion pulses is that the deleterious effects of B_1 inhomogeneities and resonance offsets on the performance characteristics of the mixing sequences can be efficiently eliminated. However, in situations where inversion pulses of very short duration, e.g. 10 μs, are required the RF power requirements for obtaining satisfactory response from mixing schemes based on adiabatic pulses could also become very large that is beyond the hardware limits of the spectrometer system. Additionally, it is also possible that RF pulse schemes based on adiabatic pulses need not necessarily lead to satisfactory performance (Herbst et al. 2007). On the other hand, considering the fact that B_1 inhomogeneities are not expected to be very significant in MAS probes with small rotor diameter, it is conceivable that very good tolerance to RF field inhomogeneities provided by mixing sequences based on adiabatic pulses may not be required at all at very high spinning speeds. Under these circumstances, the RF field modulation profiles of the 180° pulses need not be restricted to that of an adiabatic inversion pulse and, instead, can be tailored to achieve efficient mixing. What is needed is a convenient approach that takes into account the available RF power and permits the design of broadband inversion and refocussing pulses of required duration and mixing sequences based on such pulses. It is shown here that by defining the RF field modulation profiles of the 180° pulses in terms of a simple Fourier series and finding the optimal values for the Fourier coefficients it is possible to generate tailor-made 180° pulses and mixing sequences for ^{13}C–^{13}C chemical shift correlation in rotating solids.

Numerical and experimental procedures

In this study, mixing sequences were implemented with phase modulated 180° pulses with constant amplitude. The phase modulation profile, as in our recent solution state NMR studies (Kirschstein et al. 2008a, b), was expressed as a cosine Fourier series: $\varphi(t) = \Sigma a_n \cos(n\omega t)$, where $\omega = 2\pi/t_p$ is the modulation frequency with t_p corresponding to the pulse duration. RF field strength in the range of 100–120 kHz, pulsewidths in the range of 10–30 μs, limited B_1 field inhomogeneities ($< \pm 10\%$) and 6 Fourier coefficients were considered for generating broadband 180° pulses. A variety of numerical procedures such as the optimal control theory based design of excitation and inversion pulses (Kobzar et al. 2004) have been

reported in the literature. In this work, the iterative search procedure "genetic algorithms" (GA) (Goldberg 1989; Forrest 1993; Judson 1997; Haupt and Haupt 2004) that has already been used for RF pulse design in NMR (Freeman and Wu 1987; Wu and Freeman 1989; Xu et al. 1992) was employed for the numerical optimisation of the Fourier coefficients. GA employs techniques inspired by evolutionary biology, such as selection, crossover and mutation, in finding optimal solutions to complex problems. GA is a population-based approach that explores the search space in multiple directions simultaneously and applies the principle of survival of the fittest to produce better and better approximations to a solution. In brief, many individual solutions, covering the entire range of possible solutions, are generated randomly to form the initial population/input for the GA. Starting from this, GA evolves to find the optimal solution over several generations. In each generation, the fitness/performance characteristic of every candidate solution in the population is evaluated. The best-performing candidate solutions are selected, based on their fitness, for breeding the next generation of population through genetic operators. The combined application of selection, crossover and mutation generally leads to improving fitness values in consecutive populations. The generational process is repeated until a fixed number of iterations are carried out or an optimal solution is found. In this study, the "GAsimpleGA" routine from the GAlib genetic algorithm program package written by Matthew Wall at the Massachusetts Institute of Technology (Wall 1996) was employed. Typically, 250–500 generations and a population size in the range of 1,000–10,000 were used. Each candidate solution in the population was represented as a one dimensional array of real numbers. The roulette wheel selection method (Goldberg 1989; Judson 1997; Haupt and Haupt 2004) was employed as the reproduction operator for selecting elitist individuals. Single-point crossover and swap mutator genetic operators were employed for going from one generation to the next. Considering a simple spin 1/2 system, the broadband inversion and refocussing pulses were generated so as to obtain the required response, $\langle I_z \rangle \rightarrow -\langle I_z \rangle$, and propagator, $\exp(i\pi I_x)$, respectively. Mixing sequences based on these GA derived pulses were implemented for generating dipolar and scalar coupling mediated chemical shift correlation spectra. The performance characteristics of the mixing sequences were first evaluated via numerical simulations. The Fourier coefficients of the RF pulses were further optimised, where needed (see below), to achieve improved mixing performance. Standard phase cycling procedures were applied to obtain phase sensitive data via longitudinal magnetisation exchange. Dipolar correlation experiments without ^{1}H decoupling during mixing were carried out at a spinning speed of 34.0 kHz via the zero-quantum dipolar recoupling sequence RFDR (Bennett et al. 1992, 1998; Ishii 2001). The scalar coupling mediated experiments were carried out at a MAS frequency of 33.333 kHz via CN_n^{ν} symmetry-based RF pulse schemes. All spectra were generated with a ^{15}N, ^{13}C labelled polycrystalline sample of L-histidine hydrochloride monohydrate (98% labelling) as obtained from Cambridge Isotope Laboratories. A 500 MHz wide-bore Bruker Avance III solid state NMR spectrometer equipped with a 2.5 mm triple resonance probe with the cooling air kept at a temperature of ~ -50°C (corresponding to a sample temperature of ~ 0°C) was employed. All multi-spin numerical simulations and optimisation calculations were carried out with the SPINEVOLUTION program (Veshtort and Griffin 2006) using typical chemical shift, scalar and dipolar coupling parameters as in our earlier studies (Leppert et al. 2003). All simulations employed 168 α and β powder angles selected according to the REPULSION (Bak and Nielsen 1997) scheme and 16 γ angles.

Results and discussion

The Fourier coefficients a_n, the phase modulation as well as the corresponding frequency sweep profiles and simulated inversion characteristics of a few *representative*, high-power broadband 180° pulses with durations in the range of 10–30 μs that were generated in this study are given in Figs. 1–3. The data corresponding to 180° pulses that were designed with RF field strengths of 100 and 120 kHz for inversion of longitudinal magnetisation over a bandwidth of 100 and 200 kHz, respectively, are given in Figs. 1 and 2. The plots for universal rotors/refocussing pulses generated with an RF field strength of 120 kHz and for an inversion bandwidth of 100 kHz are shown in Fig. 3. Under minor variations in the RF field strength, e.g. in the presence of RF field inhomogeneities, the performance of the 180° pulses are found typically to be not affected significantly. Many of the inversion pulses reported here show pronounced frequency swings, especially at the edges. The phase modulated pulses were divided into 100 slices of equal duration and typically it was possible to generate these pulses within a short time of a few hours using a Mac Pro with 4 cores. Although the 180° pulses were constructed for a specific duration, the phase modulated pulses are, as in the case of conventional pulses, scalable. A pulse applied for twice the duration would require half the RF field strength and correspondingly cover half the bandwidth of the original pulse. The minimum RF field strength required to achieve the desired inversion bandwidth is expected to vary as a function of the pulse duration and has not been assessed in this study. However, the data in Figs. 1–3 indicate that using RF field strengths in the range

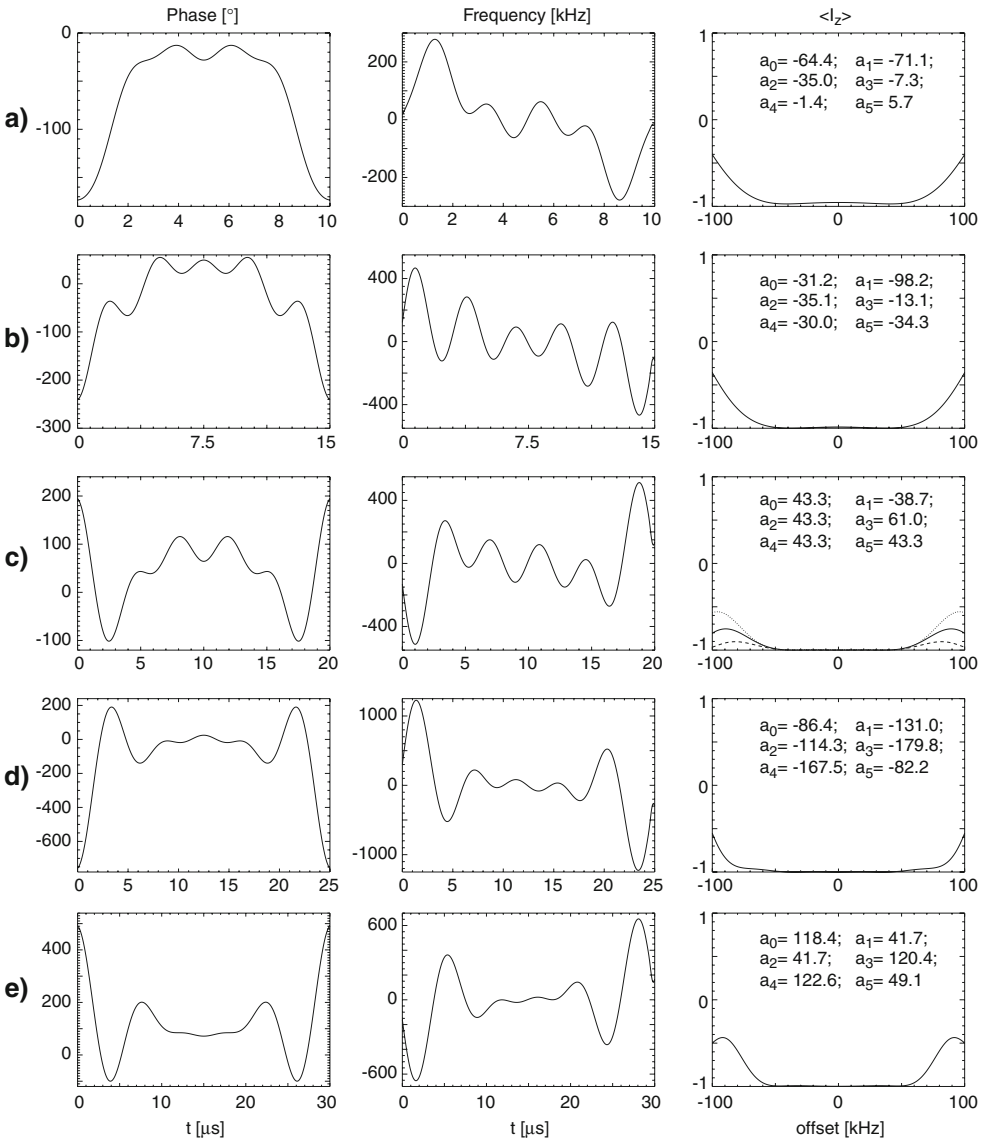

Fig. 1 The phase and the corresponding calculated frequency modulation-profiles of the 180° pulses generated considering an RF field strength of 100 kHz and an inversion bandwidth of 100 kHz. The Fourier coefficients and the longitudinal magnetisation inversion characteristics of the different pulses are also given. As a representative case, the inversion performance observed for ±10% variation in the RF field strength is also given for the 180° pulse of 20 µs duration

of 100–120 kHz, that is typically available in high MAS solid state NMR probes, short, high-power broadband 180° pulses can be conveniently designed for efficiently achieving $\langle I_z\rangle \rightarrow -\langle I_z\rangle$ as well as for inverting both the z and y magnetisation components.

Mixing sequences were generated using phase modulated inversion and refocussing pulses and the performance characteristics were assessed numerically by considering heteronuclear ^{13}C–^{1}H dipolar couplings in either a four-spin $^{1}H1$–$^{13}C1$–$^{13}C2$–$^{1}H2$ or three-spin $^{1}H1$–$^{13}C1$–$^{13}C2$ system. In general, the magnitude of longitudinal magnetisation transferred to the second carbon spin ($^{13}C'/^{13}C^{\beta}$) as a function of the mixing time, starting with z magnetisation on the first carbon spin ($^{13}C^{\alpha}$) at zero mixing time was studied. The initial rate of transfer of magnetisation from one spin to another, which is a measure of the effectiveness of the sequence, with a faster transfer representing a more efficient mixing, was monitored. Some of the phase modulated 180° pulses were found to lead to satisfactory performance without requiring any further optimisation of the Fourier coefficients. Figure 4 shows the RFDR performance at a spinning speed of 34 kHz and under the rotor-synchronised application of one 10 µs phase modulated inversion pulse at the centre of each rotor period with the *xy*-16 (Gullion et al. 1990) phasing scheme. Simulations are given for two representative Zeeman field strengths corresponding to ^{1}H frequencies of 500 and 750 MHz. For comparison, the performances observed with 5 and 10 µs rectangular 180° pulses are also shown. As seen from these plots, RFDR with the phase modulated pulse leads to a better overall performance, especially at 750 MHz. The magnetisation transfer characteristics with the phase modulated pulse is also found to be better compared to that of a 5 µs pulse when the two carbon

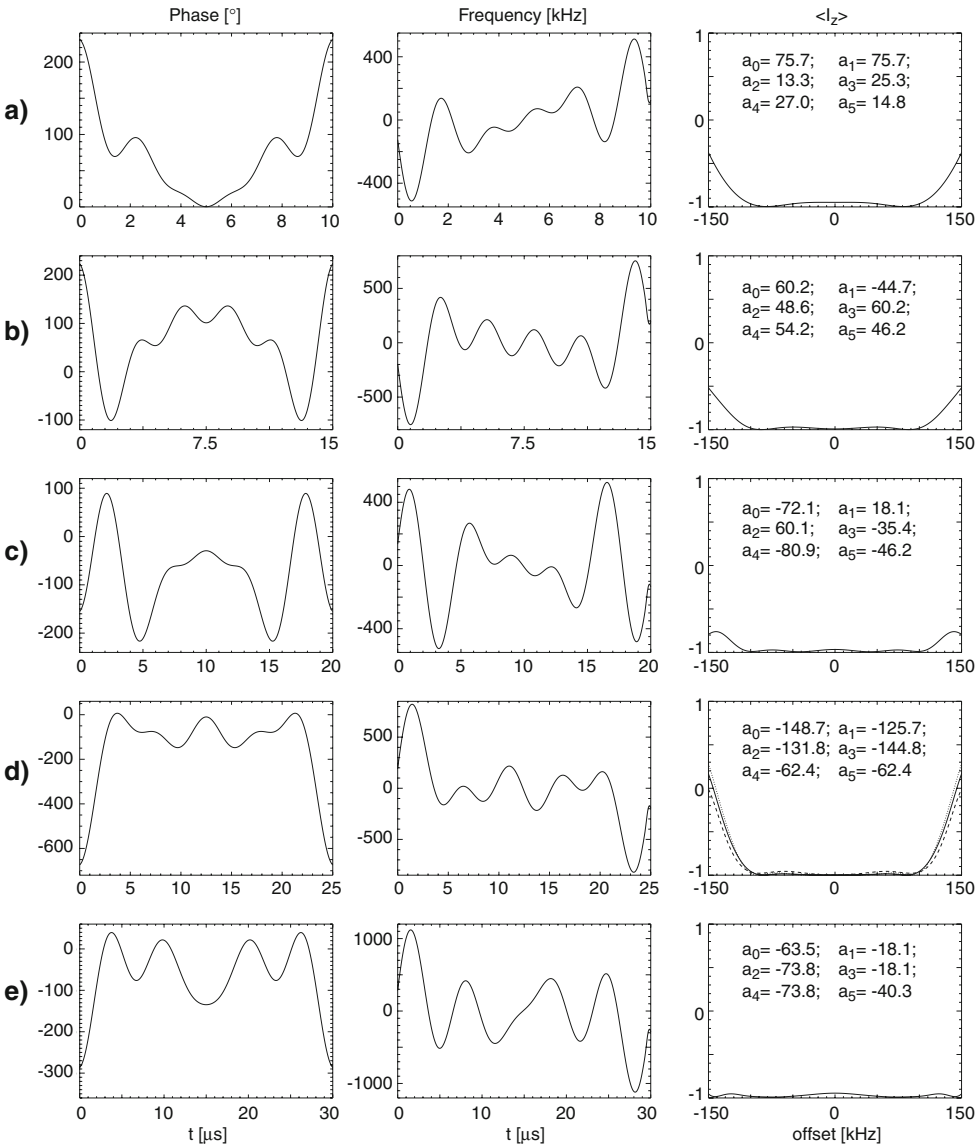

Fig. 2 The phase and the corresponding frequency modulation-profiles of the 180° pulses generated considering an RF field strength of 120 kHz and an inversion bandwidth of 200 kHz. The Fourier coefficients and the longitudinal magnetisation inversion characteristics of the different pulses are also given. As a representative case, the inversion performance observed for ±10% variation in the RF field strength is also given for the 180° pulse of 25 μs duration

nuclei have large CSAs and when the isotropic chemical shift difference between these nuclei is not very large, as is typically the case with carbons in the aromatic rings (data not shown).

A variety of CN_n^v symmetry-based RF pulse schemes, such as the $C9_{15}^1$ mixing scheme mentioned earlier, have been proposed in the literature for the selection of homonuclear *J*-couplings with suppression of all homonuclear DD couplings and CSA terms. Such sequences can also be employed, in principle, in the absence of ^{1}H decoupling during mixing. An initial assessment of the TOBSY performance characteristics of CN_n^v symmetry-based RF pulse schemes using phase modulated 180° pulses was carried out via numerical simulations. The magnetisation transfer characteristics observed in the four spin ^{1}H1–^{13}C1–^{13}C2–^{1}H2 system, considering heteronuclear dipolar couplings explicitly, were found to be far from satisfactory. Hence, further optimisation of the RF phase-modulation profile was undertaken to achieve efficient mixing. Considering a representative spinning speed of 33.333 kHz, phase modulated 180° pulses of 25 μs duration and a basic *C* element of the type $\{x\bar{x}\}$, the numerical calculations were carried out so as to achieve efficient TOBSY performance via the $C9_{15}^1$ symmetry-based RF pulse scheme. The nonlinear least-squares optimisation procedure NL2SOL implemented in the SPINEVOLUTION program was employed to achieve complete magnetisation transfer at $\tau_{mix} = (1/2J_{cc})$ from one carbon to another in the four spin network. A Zeeman field strength corresponding to a ^{1}H resonance frequency of 500 MHz, representative scalar, dipolar and chemical shift tensor parameters of alanine and 9 Fourier coefficients were employed. To achieve an efficient broadband magnetisation transfer, the optimisation calculations were carried out to minimise the error function

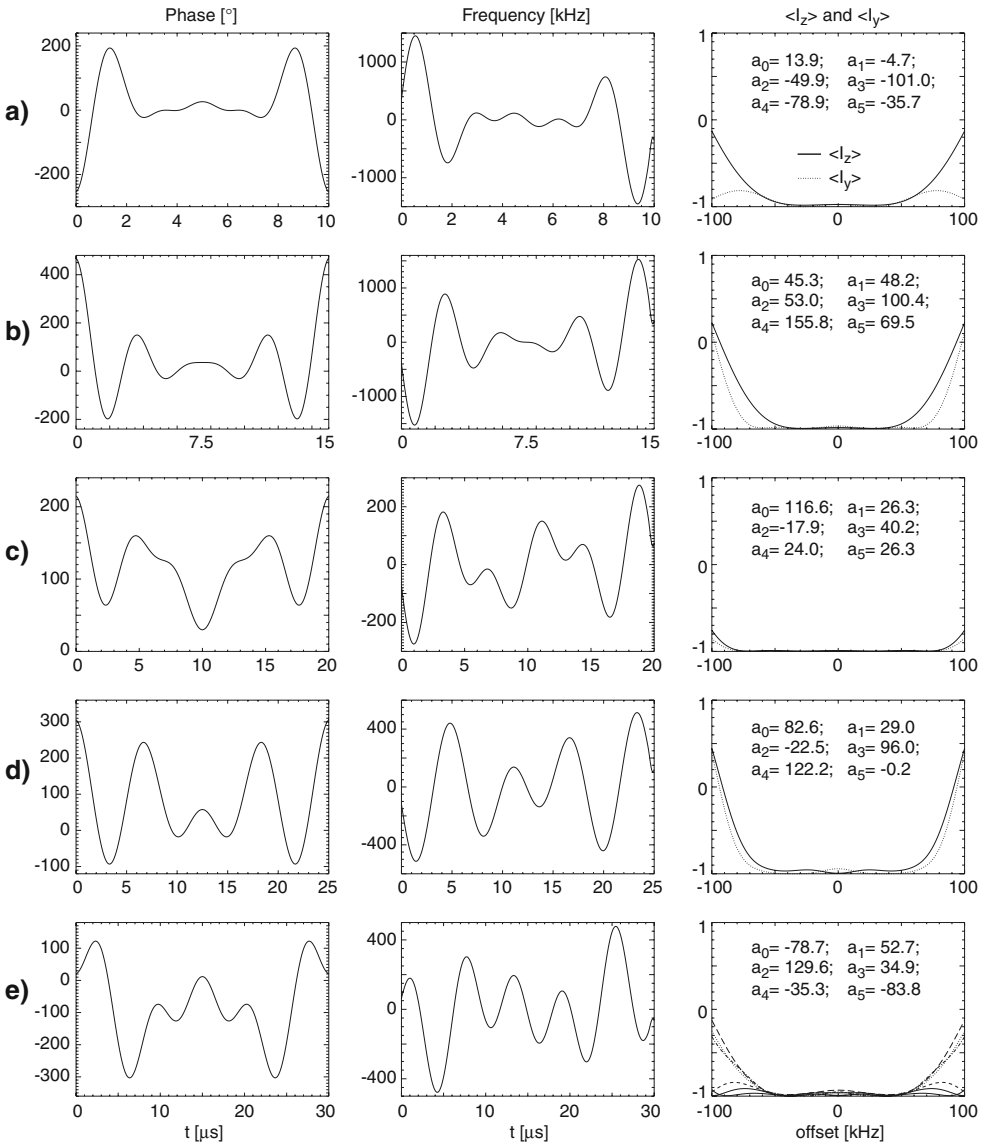

Fig. 3 The phase and the corresponding frequency modulation-profiles of the universal rotors generated considering an RF field strength of 120 kHz and an inversion bandwidth of 100 kHz. The Fourier coefficients and the longitudinal (I_z) and transverse (I_y) magnetisation inversion characteristics of the different pulses are also given. As a representative case, the inversion performance observed for ±10% variation in the RF field strength is also given for the 180° pulse of 30 μs duration

over a resonance offset range of ±15 kHz for the two carbon spins. Several optimisation runs were executed, starting with the Fourier coefficients of the inversion and refocussing pulses that led to reasonably satisfactory TOBSY performance in a simple two spin ^{13}C1–^{13}C2 system. A single stage optimisation considering the full ^{13}C–^{1}H dipolar coupling strength (set to 20 kHz, corresponding to a ^{13}C–^{1}H distance of ∼1.14 Å, in this study) was found to be less effective in arriving at good mixing sequences. Hence, to achieve satisfactory mixing in the four spin system, the ^{13}C–^{1}H dipolar coupling strength was raised gradually in several steps: 0, 2, 5, 10, 15 and 20 kHz. At every stage, to arrive at the best possible set of optimised Fourier coefficients, the local optimisation run was repeated several times (40 in this study) varying all the Fourier coefficients randomly over a range of ±10%. The best possible set of Fourier coefficients obtained at the end of every stage were used as the starting values for the subsequent stage of optimisation. These calculations were carried out neglecting RF field inhomogeneities and considering only a limited number of 32 crystallite orientations selected according to the Zaremba–Cheng–Wolfsberg (ZCW) method (Cheng et al. 1973). Typically, it was possible to carry out the optimisation calculations within a short period of 9–12 h. Increasing the number of crystallite orientations in the optimisation calculations did not lead to any significantly improved solutions.

The magnetisation transfer characteristics observed with one of the best TOBSY mixing sequences generated in this study are shown in Fig. 5, along with the phase modulation profile of the 180° pulse constituting the mixing scheme. This TOBSY mixing sequence was generated starting from a 25 μs universal rotor constructed for an inversion bandwidth of 260 kHz using an RF field strength of 120 kHz.

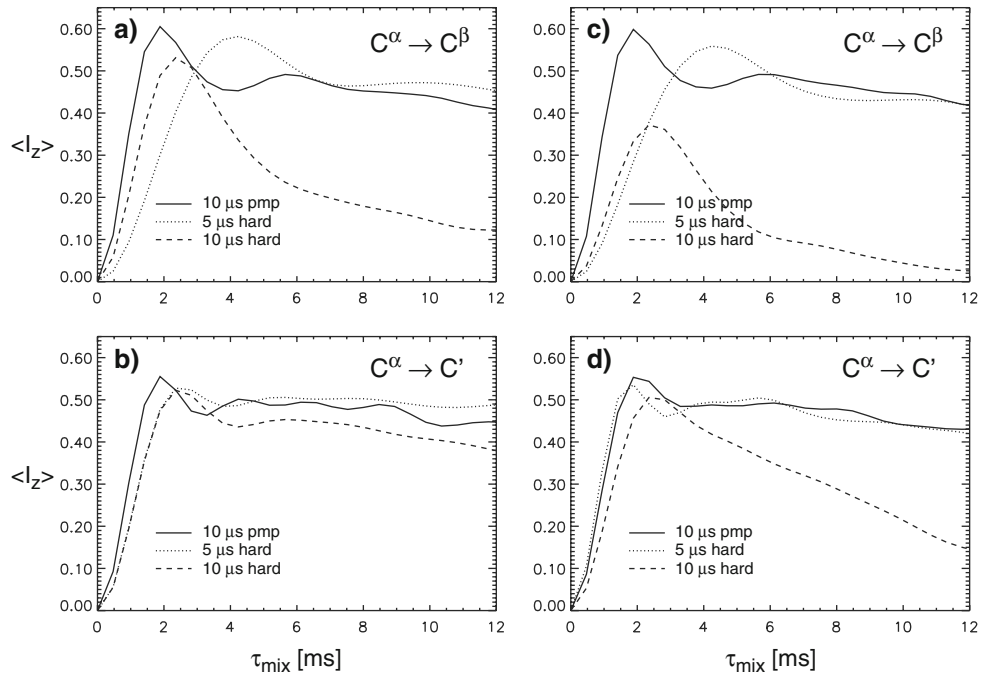

Fig. 4 Simulated longitudinal magnetisation transfer characteristics observed with the RFDR sequence at a spinning speed of 34 kHz, in the absence of ^{1}H decoupling during mixing, using phase-modulated inversion pulse of 10 µs duration and *xy*-16 phasing scheme. For comparison, the performance observed with rectangular inversion pulses of 5 and 10 µs are also given. The Fourier coefficients of the phase-modulated 10 µs pulse designed for an inversion bandwidth of 60 kHz with an RF field strength of 120 kHz are: $a_0 = -56.7$; $a_1 = 66.7$; $a_2 = 27.8$; $a_3 = 23.5$; $a_4 = -5.5$; $a_5 = -14.1$. These simulated plots show, at Zeeman field strengths corresponding to ^{1}H frequencies of 500 MHz (**a**, **b**) and 750 MHz (**c**, **d**), the magnitude of the transferred magnetisation (normalised to the maximum transferable signal) on the second carbon ($^{13}C^\beta/^{13}C'$) starting with *z* magnetisation on carbon 1 ($^{13}C^\alpha$). The simulations for the $C^\alpha \rightarrow C^\beta$ transfer were carried out considering a four spin ^{1}H1–^{13}C1–^{13}C2–^{1}H2 network (with all the atoms in the same plane) and that for the $C^\alpha \rightarrow C'$ transfer were carried out with a three spin ^{1}H1–^{13}C1–^{13}C2 network. A ^{13}C–^{1}H dipolar coupling strength of 20 kHz was employed in these simulations and the C–H bonds were assumed to be at an angle of 109° with respect to the C–C bond, corresponding to the *z* axis of the molecular frame. These simulations were carried out keeping the ^{13}C RF carrier at 110 ppm, using typical chemical shift, scalar and dipolar coupling parameters of alanine and glycine as in our earlier studies (Leppert et al. 2003)

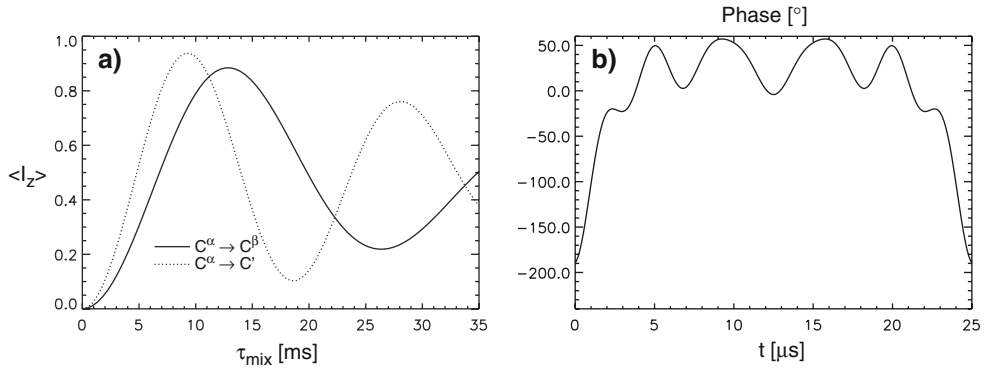

Fig. 5 Simulated longitudinal magnetisation transfer characteristics (**a**) observed with the $C9^1_{15}$ symmetry-based RF pulse scheme, using a basic C element of the type {x$\bar{x}$}, 180° pulses of 25 µs duration with optimised phase-modulation profile given in (**b**). Simulations were carried out at a spinning speed of 33.333 kHz, for a Zeeman field strength corresponding to a ^{1}H resonance frequency of 500 MHz, in the absence of ^{1}H decoupling and with an RF field strength of 120 kHz during mixing. The Fourier coefficients of the optimised phase-modulated pulse are: $a_0 = 0.0$; $a_1 = -56.9$; $a_2 = -43.6$; $a_3 = -21.2$; $a_4 = -29.3$; $a_5 = 2.6$; $a_6 = -12.5$; $a_7 = -18.0$; $a_8 = -12.2$. The simulated plots show the magnitude of the transferred magnetisation (normalised to the maximum transferable signal) on the second carbon ($^{13}C^\beta/^{13}C'$) starting with *z* magnetisation on carbon 1 ($^{13}C^\alpha$). The simulations for the $C^\alpha \rightarrow C^\beta$ and $C^\alpha \rightarrow C'$ transfers were carried out as in the dipolar case, Fig. 4

Although we have been able to successfully generate several TOBSY mixing sequences with satisfactory performance characteristics (data not shown), an extensive search of the best possible sequence and the minimum RF field strength required at the spinning speed of 33.333 kHz has not been carried out. This would involve a detailed assessment of a variety of symmetry-based schemes employing different basic elements. This is beyond the scope of this initial study. However, the results from numerical simulations, Fig. 5, clearly demonstrate the possibilities to design at high MAS frequencies symmetry-based mixing sequences for generating scalar coupling mediated ^{13}C–^{13}C chemical shift correlation data without ^{1}H decoupling during mixing.

In addition to numerical simulations, the performance characteristics of the phase modulated mixing schemes were also assessed via experimental measurements, Figs. 6 and 7. The ^{13}C–^{13}C dipolar correlation spectrum of histidine recorded with the RFDR sequence without ^{1}H decoupling during mixing employing a spinning speed of 34 kHz, phase modulated inversion pulses of 10 µs duration, *xy*-16 phasing scheme and a mixing time of 96 rotor periods is shown in Fig. 6. For comparison, the dipolar correlation experiment was also carried out using 5 µs rectangular 180° pulses. A spectral region from these data sets is also given in Fig. 6. Consistent with the results from numerical simulations, direct and relayed crosspeaks of higher intensities are seen in the spectrum collected with

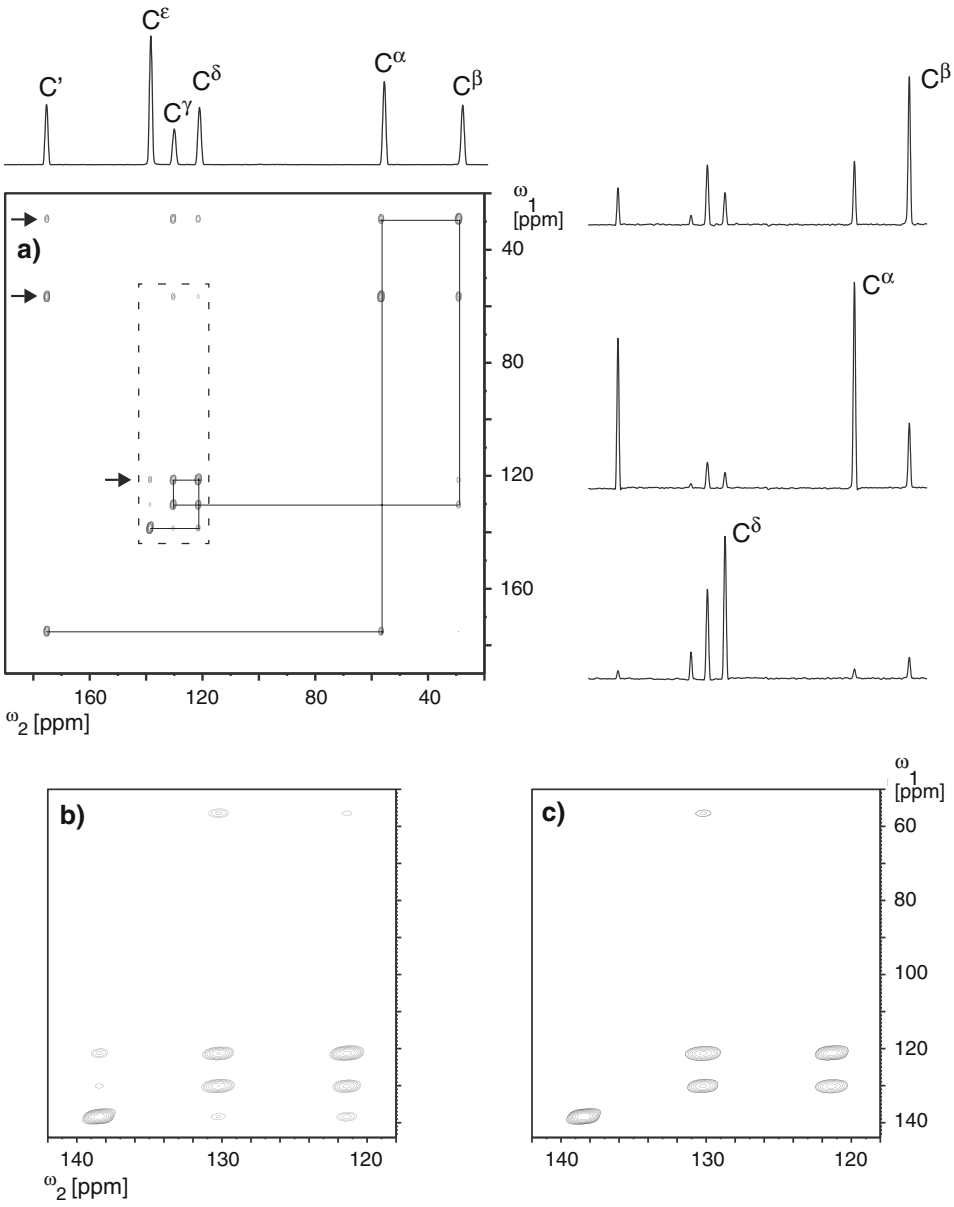

Fig. 6 **a** 2D ^{13}C–^{13}C dipolar coupling mediated chemical shift correlation spectrum obtained at a spinning speed of 34 kHz without ^{1}H decoupling and with ^{13}C RF field strength of 120 kHz during mixing. The spectrum was generated using the RFDR sequence employing 10 µs phase modulated inversion pulses (designed for an inversion bandwidth of 60 kHz with an RF field strength of 120 kHz), with 16 transients per t_1 increment, 128 t_1 increments, spectral width in the indirect dimension of 34,000 Hz and recycle time of 2 s. The *xy*-16 phasing scheme was used with a mixing time of 2.82 ms, keeping the RF carrier at 110 ppm. The base contour level was chosen at 4.8% of the maximum intensity and contours were plotted with an incrementation factor of 1.4. A few representative cross-sections are also given to indicate spectral quality. An expanded plot of the spectral region indicated is shown in Fig. 6b along with the corresponding region taken from the spectrum generated employing 5 µs rectangular inversion pulses, Fig. 6c

phase modulated inversion pulses. It is worth mentioning that RFDR can be effectively carried out with 180° pulses of duration (τ_p) comparable or equal to the rotor period (τ_r). However, when employing RF pulses of constant amplitude, it is advantageous to apply pulses of duration $\tau_p < \tau_r$ for minimising the RF heating of the sample. With such pulses of short duration, as the magnetisation spends most of the time along the z axis in a longitudinal magnetisation exchange experiment, the relaxation losses are also expected to get reduced (Herbst et al. 2007). The results presented here clearly show that phase modulated 180° pulse of short duration can be effectively employed in implementing ^{13}C–^{13}C dipolar coupling mediated chemical shift correlation experiments at very high spinning speeds. The TOBSY spectrum shown in Fig. 7 was generated at a spinning speed of 33.333 kHz using the $C9^{1}_{15}$ symmetry-based RF pulse scheme with a mixing time of 5.4 ms. Direct and relayed crosspeaks of appreciable intensities could be clearly seen in the spectrum. As reflected by the corresponding crosspeak intensities, there is significant transfer of magnetisation arising from the strong $^{13}C^{\alpha}$–$^{13}C'$ and $^{13}C^{\gamma}$–$^{13}C^{\delta}$ scalar couplings, even at the short τ_{mix} employed. Additionally, the spectrum is also essentially free from crosspeaks involving the $^{13}C^{\varepsilon}$ carbon of histidine. Consistent with the results from numerical simulations, it is seen that phase modulated mixing schemes can also be effectively employed in generating TOBSY spectra at fast MAS frequencies.

In conclusion, the present study demonstrates the possibilities to construct, taking into account the available RF power, high-power, broadband phase modulated inversion and refocussing pulses of a required duration using global optimisation procedures such as genetic algorithms. Although only a limited space of possible pulse shapes is explored by defining the RF field modulation profiles as a Fourier series, such an approach appears to be good enough to generate useful 180° pulses and mixing sequences in a relatively short period of time. For a given RF field strength and pulse duration, the largest inversion bandwidth possible is not known a priori. Hence, it is necessary to carry out several optimisation calculations considering different inversion bandwidths to find the maximum bandwidth at which satisfactory inversion performance can be realised. Employing RF field strength in the range of 100–120 kHz, it is observed that efficient phase modulated 180° pulses with inversion bandwidth of >100 kHz can be generated. The broadband 180° pulses reported here were designed in the context of implementing scalar and dipolar coupling mediated magnetisation transfers in the absence of ^{1}H decoupling during mixing. However, many of the pulses have >95% inversion efficiency and, hence, can also be effectively employed in situations where only a single

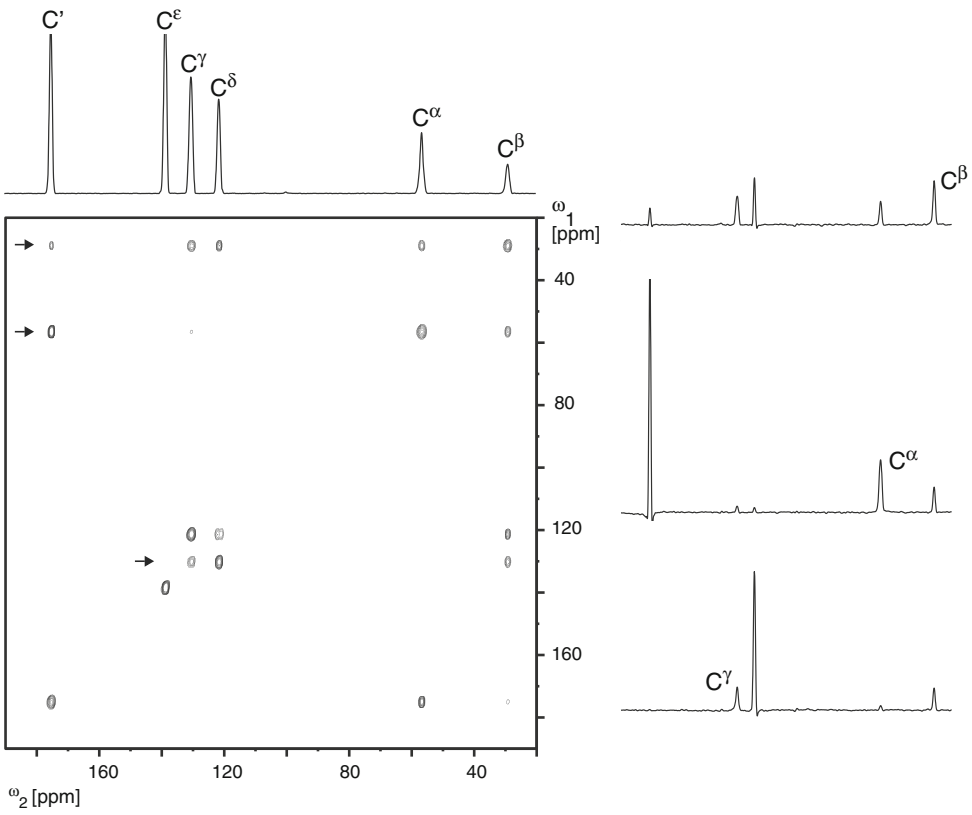

Fig. 7 2D ^{13}C–^{13}C scalar coupling mediated chemical shift correlation spectrum obtained at a spinning speed of 33.333 kHz without ^{1}H decoupling and with ^{13}C RF field strength of 120 kHz during mixing. The spectrum was generated with the $C9^{1}_{15}$ symmetry-based RF pulse scheme, using a basic C element of the type {x$\bar{x}$}, 180° pulses of 25 μs duration with optimised phase-modulation profile given in Fig. 5, 16 transients per t_1 increment, 128 t_1 increments, spectral width in the indirect dimension of 33,333 Hz and recycle time of 2 s. A mixing time of 5.4 ms was employed and the RF carrier was kept at 110 ppm. The base contour level was chosen at 1.6% of the maximum intensity and contours were plotted with an incrementation factor of 1.8. A few representative cross-sections are also given to indicate spectral quality

inversion or refocussing pulse is required. Besides the GA approach employed here, other global optimisation schemes such as simulated annealing have also been found to be equally effective for the construction of broadband, phase modulated 180° pulses. At fast MAS frequencies, it has also been shown that dipolar and scalar coupling mediated magnetisation transfers can be effectively achieved in the absence of heteronuclear decoupling during mixing via symmetry-based RF pulse schemes, making use of all the RF power available. In situations where the performance of a mixing sequence based on 180° pulses derived via the GA procedure is not satisfactory, the present work clearly demonstrates that the RF field modulation profile of the pulses can be tailored to realise efficient mixing. The method outlined here can be easily adapted for implementing other mixing sequences, e.g. homonuclear double-quantum recoupling. Although it would be computationally time consuming, several extensions to the present approach can be conceived; e.g. mixing sequences can be designed (i) taking into account explicitly RF field inhomogeneities, if any, (ii) using amplitude- and phase-modulated pulses to reduce the RF duty factor, (iii) minimising relaxation losses and (iv) representing the RF field modulation profiles simply as a list of phases and amplitudes. It may also be possible to find, in a reasonable amount of time, efficient mixing sequences via GA itself employing a heuristically guided search of the parameter space. Work in all these directions are currently in progress.

Acknowledgments This study has been funded in part by a grant from the Deutsche Forschungsgemeinschaft (GO474/6-1). The FLI is a member of the Science Association "Gottfried Wilhelm Leibniz" (WGL) and is financially supported by the Federal Government of Germany and the State of Thuringia. We would like to thank the referees for their useful comments on the original manuscript.

References

Bak M, Nielsen NC (1997) REPULSION, a novel approach to efficient powder averaging in solid state NMR. J Magn Reson 125:132–139

Baldus M, Meier BH (1996) Total correlation spectroscopy in the solid state. The use of scalar couplings to determine the through-bond connectivity. J Magn Reson A 121:65–69

Bayro MJ, Ramachandran R, Caporini MA, Eddy MT, Griffin RG (2008) Radio frequency-driven recoupling at high magic-angle spinning frequencies: homonuclear recoupling sans heteronuclear decoupling. J Chem Phys 128:052321

Bennett AE, Ok JH, Griffin RG, Vega S (1992) Chemical shift correlation spectroscopy in rotating solids: radio frequency-driven dipolar recoupling and longitudinal exchange. J Chem Phys 96:8624–8627

Bennett AE, Rienstra CM, Griffiths JM, Zhen W, Lansbury PT, Griffin RG (1998) Homonuclear radio frequency-driven recoupling in rotating solids. J Chem Phys 108:9463–9479

Castellani F, van Rossum B, Diehl A, Schubert M, Rehbein K, Oschkinat H (2002) Structure of a protein determined by solid-state magic-angle-spinning NMR spectroscopy. Nature 420: 98–102

Cheng VB, Suzukawa HH, Wolfsberg M (1973) Investigations of a nonrandom numerical method for multidimensional integration. J Chem Phys 59:3992–3999

Detken A, Hardy EH, Ernst M, Kainosho M, Kawakami T, Aimoto S, Meier BH (2001) Methods for sequential resonance assignment in solid, uniformly ^{13}C, ^{15}N labelled peptides: quantification and application to antamanide. J Biomol NMR 20:203–221

De Paepe G, Bayro MJ, Lewandowski J, Griffin RG (2005) Broadband homonuclear correlation spectroscopy at high magnetic fields and MAS frequencies. J Am Chem Soc 128: 1776–1777

Ernst M, Detken A, Bockmann A, Meier BH (2003) NMR spectra of a microcrystalline protein at 30 kHz MAS. J Am Chem Soc 125:15807–15810

Forrest S (1993) Genetic algorithms—principles of natural-selection applied to computation. Science 261:872–878

Freeman R, Wu XL (1987) Design of magnetic resonance experiments by genetic evolution. J Magn Reson 75:184–189

Goldberg DE (1989) Genetic algorithms in search, optimization and machine learning. Addison-Wesley publishing company, Massachusetts

Goldbourt A, Gross BJ, Day LA, McDermott AE (2007) Filamentous phage studied by magic-angle spinning NMR: resonance assignment and secondary structure of the coat protein in Pf1. J Am Chem Soc 129:2338–2344

Gullion T, Baker DB, Conradi MS (1990) New, compensated Carr-Purcell sequences. J Magn Reson 89:479–484

Hardy EH, Detken A, Meier BH (2003) Fast-MAS total through-bond correlation spectroscopy using adiabatic pulses. J Magn Reson 165:208–218

Haupt RL, Haupt SE (2004) Practical genetic algorithms. Wiley-Interscience, Hoboken, New Jersey

Heindrichs ASD, Geen H, Giordani C, Titman JJ (2001) Improved scalar shift correlation NMR spectroscopy in solids. Chem Phys Lett 335:89–96

Herbst C, Riedel K, Leppert J, Ohlenschläger O, Görlach M, Ramachandran R (2007) ^{13}C–^{13}C chemical shift correlation in rotating solids without ^{1}H decoupling during mixing: an assessment of amplitude and phase-modulated adiabatic RF pulse schemes. Chem Phys Chem 8:1770–1773

Hughes CE, Luca S, Baldus M (2004) Radio-frequency driven polarization transfer without heteronuclear decoupling in rotating solids. Chem Phys Lett 385:435–440

Ishii Y (2001) ^{13}C–^{13}C dipolar recoupling under very fast magic angle spinning in solid-state nuclear magnetic resonance: applications to distance measurements, spectral assignments, and high-throughput secondary-structure determination. J Chem Phys 114:8473–8483

Jaroniec CP, MacPhee CE, Astrof NS, Dobson CM, Griffin RG (2002) Molecular conformation of a peptide fragment of transthyretin in an amyloid fibril. Proc Natl Acad Sci USA 99:16748–16753

Judson R (1997) Genetic algorithms and their use in chemistry. In: Lipkowitz KB, Boyd DB (eds) Reviews in computational chemistry, vol 10. VCH Publishers, New York, pp 1–73

Kirschstein A, Herbst C, Riedel K, Carella M, Leppert J, Ohlenschläger O, Görlach M, Ramachandran R (2008a) Broadband homonuclear TOCSY with amplitude and phase-modulated RF mixing schemes. J Biomol NMR 40:227–237

Kirschstein A, Herbst C, Riedel K, Carella M, Leppert J, Ohlenschläger O, Görlach M, Ramachandran R (2008b) Heteronuclear *J*

cross-polarisation in liquids using amplitude and phase modulated mixing sequences. J Biomol NMR 40:277–283

Kobzar K, Skinner TE, Khaneja N, Glaser SJ, Luy B (2004) Exploring the limits of broadband excitation and inversion pulses. J Magn Reson 170:236–243

Krabben L, van Rossum BJ, Castellani F, Bocharov E, Schulga AA, Arseniev AS, Weise C, Hucho F, Oschkinat H (2004) Towards structure determination of neurotoxin II bound to nicotinic acetylcholine receptor: a solid state NMR approach. FEBS Lett 564:319–324

Leppert J, Heise B, Ohlenschläger O, Görlach M, Ramachandran R (2003) Broadband RFDR with adiabatic inversion pulses. J Biomol NMR 26:13–24

Leppert J, Urbinati CR, Häfner S, Ohlenschläger O, Swanson MS, Görlach M, Ramachandran R (2004) Identification of NH…N hydrogen bonds by magic angle spinning solid state NMR in a double-stranded RNA associated with myotonic dystrophy. Nucleic Acids Res 32:1177–1183

Levitt MH (2002) Symmetry-based pulse sequences in magic-angle spinning solid-state NMR. In: Grant DM, Harris RK (eds) Encyclopedia of nuclear magnetic resonance. John Wiley, Chichester, New York

Luca S, White JF, Sohal Ak, Filippov DV, van Boom JH, Grisshammer R, Baldus M (2003) The conformation of neurotinsin bound to its G protein-coupled receptor. Proc Natl Acad Sci USA 100:10706–10711

Marin-Montesinos I, Brouwer DH, Antonioli G, Lai WC, Brinkmann A, Levitt MH (2005) Heteronuclear decoupling interference during symmetry-based homonuclear recoupling in solid-state NMR. J Magn Reson 177:307–317

Mou Y, Chao JCH, Chan JCC (2006) Efficient spin–spin scalar coupling mediated ^{13}C homonuclear polarization in biological solids without proton decoupling. Solid State Nucl Magn Reson 29:278–282

Rienstra CM, Tucker-Kellog L, Jaroniec CP, Hohwy M, Reif B, McMahon MT, Tidor B, Lozano-Perez T, Griffin RG (2002) De novo determination of peptide structure with solid-state magic-angle spinning NMR spectroscopy. Proc Natl Acad Sci USA 99:10260–10265

Riedel K, Leppert J, Ohlenschläger O, Görlach M, Ramachandran R (2005) Characterisation of hydrogen bonding networks in RNA via magic angle spinning solid state NMR spectroscopy. J Biomol NMR 31:331–336

Riedel K, Herbst C, Häfner S, Leppert J, Ohlenschläger O, Swanson MS, Görlach M, Ramachandran R (2006) Constraints on the structure of $(CUG)_{97}$ RNA from magic-angle-spinning solid-state NMR spectroscopy. Angew Chem Int Ed 45:5620–5623

Riedel K, Herbst C, Leppert J, Ohlenschläger O, Görlach M, Ramachandran R (2007) Broadband homonuclear chemical shift correlation at high MAS frequencies: a study of tanh/tan adiabatic RF pulse schemes without ^{1}H decoupling during mixing. J Biomol NMR 37:277–286

Tycko R (2003) Application of solid state NMR to the structural characterization of amyloid fibrils: methods and results. Prog Nucl Magn Reson Spectrosc 42:53–68

Veshtort M, Griffin RG (2006) SPINEVOLUTION: a powerful tool for the simulation of solid and liquid state NMR experiments. J Magn Reson 178:248–282

Wall M (1996) GAlib: a C++ Library of genetic algorithm components, version 2.4.7

Wu XL, Freeman R (1989) Darwin's ideas applied to magnetic resonance. The marriage broker. J Magn Reson 85:414–420

Xu P, Wu XL, Freeman R (1992) User-friendly selective pulses. J Magn Reson 99:308–322

Zech SG, Wand AJ, McDermott AE (2005) Protein structure determination by high-resolution solid state NMR spectroscopy: application to microcrystalline ubiquitin. J Am Chem Soc 127:8618–8626

Zhou DH, Shea JJ, Nieuwkoop AJ, Franks WT, Wylie BJ, Mullen C, Sandoz D, Rienstra CM (2007) Solid-state protein-structure determination with proton-detected triple-resonance 3D magic-angle-spinning NMR spectroscopy. Angew Chem Int Ed 46:8380–8383